Search for Spatially Extended *Fermi*-LAT Sources Using Two Years of Data

Joshua Lande,
Stefan Funk,
Markus Ackermann

February 15, 2012

Search for Spatially Extended *Fermi*-LAT Sources Using Two Years of Data

J. Lande[1,2], M. Ackermann[3,4], A. Allafort[1], J. Ballet[5], K. Bechtol[1], T. H. Burnett[6], J. Cohen-Tanugi[7], A. Drlica-Wagner[1], S. Funk[1,8], F. Giordano[9,10], M.-H. Grondin[11,12], M. Kerr[1], M. Lemoine-Goumard[13,14]

- Cat II paper
- Internal referees: Marianne Lemoine-Goumard + Johann Cohen-Tanugi (+ unofficially Jean Ballet)
- Submitted to ApJ

Sec. 2: Extended Sources in pointlike

- Pointlike designed for speed
  - Scale pixel size with energy
  - Sparse Matricies
  - Other optimizations in evaluating likelihood
- Implementation of extended sources in pointlike
  - Semi-Analytic Convolution to speed up calculation
- Simultaneously Fit position + extension with MINUIT
- Cross check TS + spectral values using `gtlike`

Fig. 2: LAT PSF

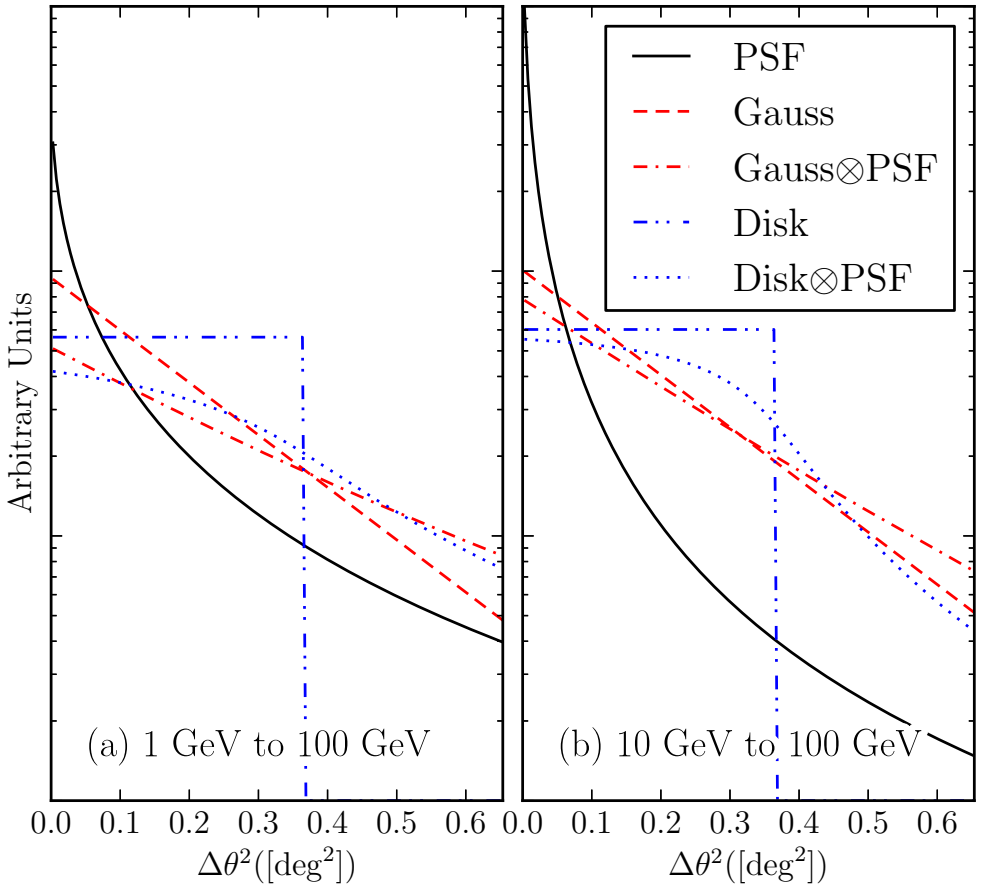

- Compare Disk, Gauss, and their convolutions with the PSF
- For smaller extended sources, little sensitivity to spatial shape

Table 1: False-Detection Rate

Table 1. Monte Carlo Spectral Parameters

Spectral Index	Flux[a] ($\mathrm{ph\,cm^{-2}\,s^{-1}}$)	$N_{1-100\mathrm{GeV}}$	$\langle \mathrm{TS} \rangle_{1-100\mathrm{GeV}}$	$N_{10-100\mathrm{GeV}}$	$\langle \mathrm{TS} \rangle_{10-100\mathrm{GeV}}$
1.5	3×10^{-7}	18938	22233	18938	8084
	10^{-7}	19079	5827	19079	2258
	3×10^{-8}	19303	1276	19303	541
	10^{-8}	19385	303	19381	142
	3×10^{-9}	18694	62	12442	43
2	10^{-6}	18760	22101	18760	3033
	3×10^{-7}	18775	4913	18775	730
	10^{-7}	18804	1170	18803	192
	3×10^{-8}	18836	224	15256	50
	10^{-8}	17060	50	...	...
2.5	3×10^{-6}	18597	19036	18597	786
	10^{-6}	18609	4738	18608	208
	3×10^{-7}	18613	954	15958	53
	10^{-7}	18658	203	...	...
	3×10^{-8}	14072	41	...	...
3	10^{-5}	18354	19466	18354	215
	3×10^{-6}	18381	4205	15973	54
	10^{-6}	18449	966	...	...
	3×10^{-7}	18517	174	...	...
	10^{-7}	13714	41	...	...

[a]Integral 100 MeV to 100 GeV flux.

- Simulate point-like sources
- Test for extension
- Good agreement with Wilk's Theorem
- Use $\sqrt{\mathrm{TS}_{\mathrm{ext}}}$ as a measure of significance
- $\sim 20,000$ Simulations per spectral model!
- Test in 1 GeV to 100 GeV + 10 GeV to 100 GeV energy range

Fig. 3+4: False-Detection Rate (cont)

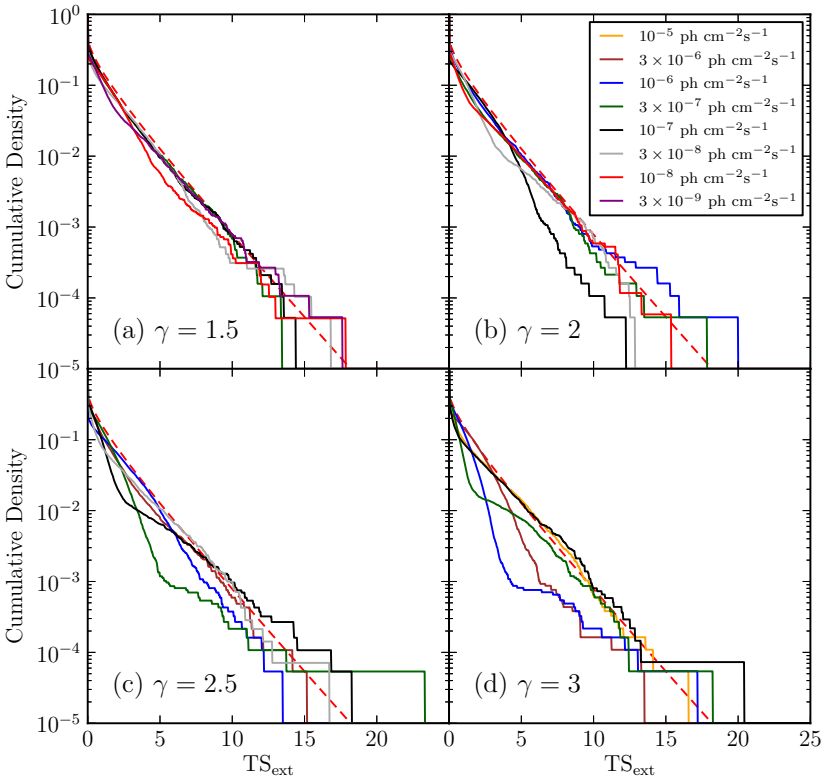

Fig 3: 1 GeV to 100 GeV

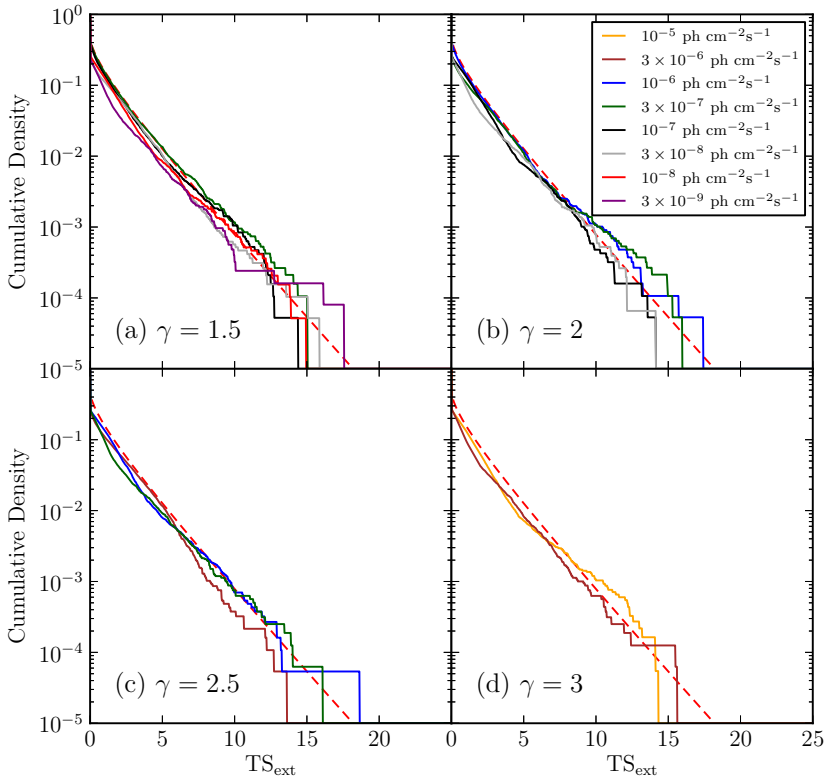

Fig 4: 10 GeV to 100 GeV

Fig. 5: Detection Threshold

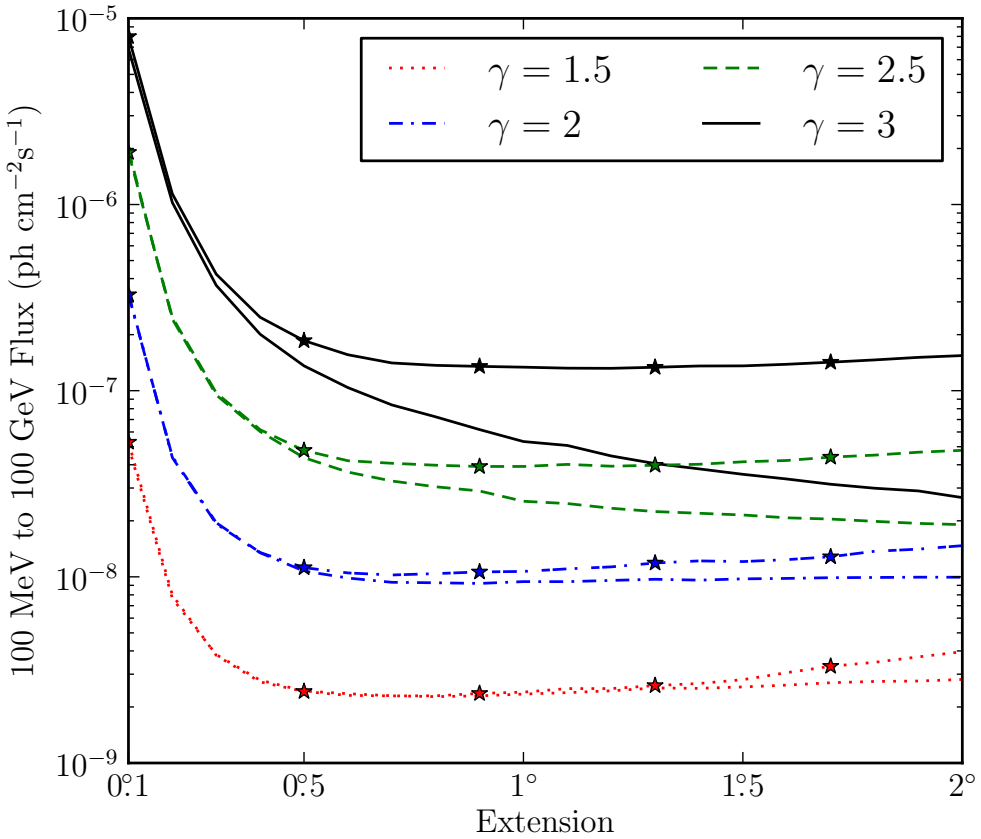

- Detetion threshold to extension
- $\langle \mathrm{TS}_{\mathrm{ext}} \rangle = 16$
- Vary spectra, background, energy range
- More sensitive to Harder sources
- Not sensitive to very small extended sources

Fig. 6: Detection Threshold (cont)

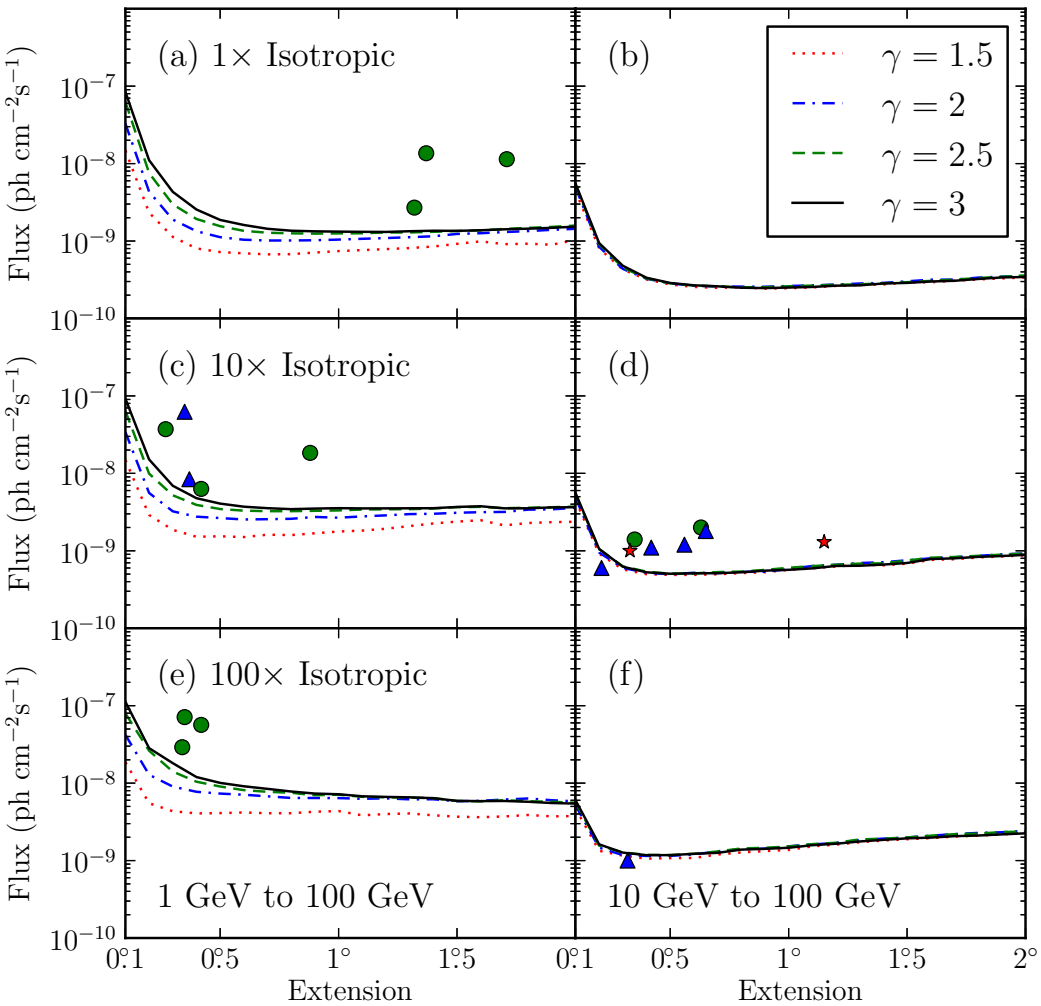

- Compute sensitivty for
  - different background levels
  - energy ranges.
  - Spectral Indices
- Little index dependence to sensitivity for hard or larger sources
- Overlay extended sources $\rightarrow$ Good we are sensitive to them

Table 2. Extension Detection Threshold

γ	BG	0.1	0.2	0.3	0.4	0.5	0.6	0.7	0.8	0.9	1.0	1.1	1.2	1.3	1.4	1.5	1.6	1.7	1.8	1.9	2.0
E>1 GeV																					
1.5	1×	148.1	23.3	11.3	8.0	7.2	6.9	6.7	6.8	7.1	7.4	7.6	7.9	8.1	8.5	9.2	9.9	9.1	9.2	9.0	10.3
	10×	148.4	29.0	18.7	15.2	15.4	15.0	16.1	16.0	16.8	17.7	18.2	19.3	20.9	22.5	23.8	24.8	21.3	22.8	23.4	23.7
	100×	186.8	55.0	43.4	40.7	41.0	41.8	40.9	40.9	42.7	43.6	38.4	39.9	40.6	38.4	36.9	36.3	37.1	38.8	37.2	37.6
2	1×	328.4	43.4	18.9	13.4	11.2	10.4	10.2	10.2	10.2	10.4	10.7	10.9	11.2	11.5	12.4	12.6	13.0	13.4	14.0	14.4
	10×	341.0	55.9	32.3	27.6	26.5	25.4	25.6	25.9	27.4	26.8	27.8	28.7	29.8	30.1	31.0	31.5	31.7	34.0	34.3	35.9
	100×	420.5	128.3	90.2	77.3	73.3	70.8	67.5	64.3	64.2	64.1	62.8	63.6	61.7	61.9	58.4	59.0	61.4	63.3	60.1	58.1
2.5	1×	627.1	75.6	29.8	19.3	15.5	13.5	12.8	12.6	12.5	12.5	12.6	12.9	12.9	13.1	13.5	13.7	14.3	14.8	15.2	15.8
	10×	638.9	99.1	52.1	39.1	34.6	33.0	32.5	32.5	32.8	33.2	34.1	34.3	34.5	35.1	36.6	36.9	35.5	36.0	36.5	37.3
	100×	795.0	262.1	140.9	104.3	90.4	81.2	77.2	75.1	69.7	70.9	66.5	65.6	64.9	64.0	58.9	58.1	60.2	58.4	57.5	55.8
3	1×	841.5	110.6	43.2	25.5	18.7	16.1	14.4	13.6	13.3	13.2	13.1	13.1	13.4	13.6	13.5	13.8	14.2	14.4	14.8	15.4
	10×	921.6	151.3	69.1	47.8	40.7	37.1	35.5	34.5	35.1	35.5	35.3	35.3	35.4	35.5	36.8	37.6	35.3	35.4	36.3	36.6
	100×	1124.1	282.9	181.1	119.8	100.7	91.1	84.3	77.9	73.3	71.8	67.6	66.4	65.5	63.9	59.0	58.6	58.8	57.5	55.4	54.4
E>10 GeV																					
1.5	1×	44.6	8.0	4.3	3.2	2.7	2.6	2.5	2.5	2.4	2.5	2.5	2.6	2.7	2.8	2.9	2.9	3.1	3.2	3.3	3.4
	10×	45.2	9.2	5.8	5.0	4.9	4.9	5.0	5.2	5.3	5.7	5.9	6.3	6.6	6.5	6.8	7.6	7.8	8.2	8.5	8.7
	100×	47.3	13.4	11.6	10.6	10.8	10.8	12.0	12.7	13.2	13.7	15.3	16.1	17.2	18.2	18.9	19.5	20.4	21.0	21.7	22.9
2	1×	49.7	8.4	4.4	3.3	2.8	2.6	2.6	2.6	2.6	2.6	2.7	2.7	2.8	2.9	3.0	3.2	3.2	3.4	3.5	3.5
	10×	48.6	9.5	6.0	5.2	5.0	5.2	5.2	5.3	5.4	5.8	6.4	6.6	7.0	7.1	7.5	8.0	8.3	8.6	9.0	9.2
	100×	51.8	14.7	11.8	11.5	11.5	11.9	13.2	14.0	14.3	15.3	16.2	16.9	18.4	19.2	19.8	21.0	22.0	22.8	23.2	24.3
2.5	1×	53.1	9.1	4.5	3.3	2.8	2.7	2.6	2.5	2.5	2.6	2.7	2.7	2.8	2.8	2.9	3.1	3.2	3.3	3.5	3.6
	10×	53.7	10.5	6.3	5.4	5.1	5.1	5.3	5.4	5.7	6.0	6.3	6.6	6.8	6.9	7.5	8.1	8.3	8.6	8.9	9.2
	100×	57.0	15.6	12.7	11.9	11.8	12.2	13.1	14.3	14.6	15.2	16.3	17.0	18.8	19.2	19.9	21.0	21.9	22.3	23.3	23.7
3	1×	55.5	9.4	4.8	3.4	2.9	2.7	2.6	2.5	2.5	2.5	2.6	2.7	2.7	2.8	2.9	3.0	3.1	3.2	3.4	3.4
	10×	56.0	10.5	6.2	5.3	5.1	5.1	5.1	5.3	5.5	5.7	5.9	6.4	6.4	6.6	7.0	7.8	8.0	8.3	8.6	8.9
	100×	60.3	16.2	12.7	11.7	11.8	12.2	12.6	13.8	14.2	14.6	15.8	16.5	17.6	18.5	19.4	19.8	20.7	21.0	21.8	22.5

Note. — The detection threshold to resolve spatially extended sources with a uniform disk spatial model for a two-year exposure The threshold is calculated for sources of varying energy ranges, spectral indices, and background levels. The sensitivity was calculated against a Sreekumar-like isotropic background and the second column is the factor that the simulated background was scaled by. The remaining columns are varying sizes of the source. The table quotes integral fluxes in the analyzed energy range (1 GeV to 100 GeV or 10 GeV to 100 GeV) in units of 10^{-10} ph cm^{-2} s^{-1}.

Fig. 7: Detection Threshold (cont)

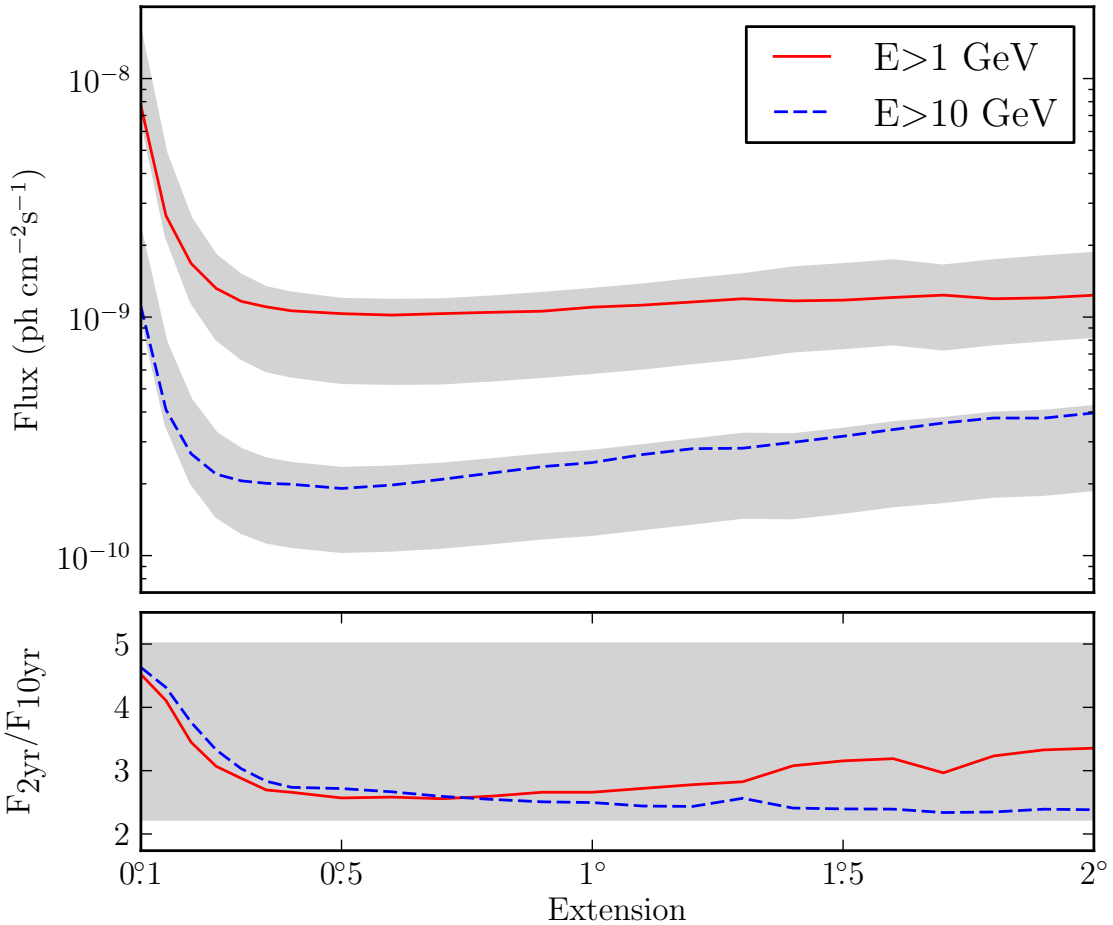

- Compute sensitivty after 10 years.
- Improvement better than $\sqrt{n}$ for small sources
- True becasue sensitivity dominated by high energy $\rightarrow$ not background limited

Fig. 8: Effects of Source Confusion

Is it an extended source or two point sources?

$$\mathrm{TS}_{\mathrm{2pts}} = 2\log(\mathcal{L}_{\mathrm{2pts}}/\mathcal{L}_{\mathrm{ps}})$$

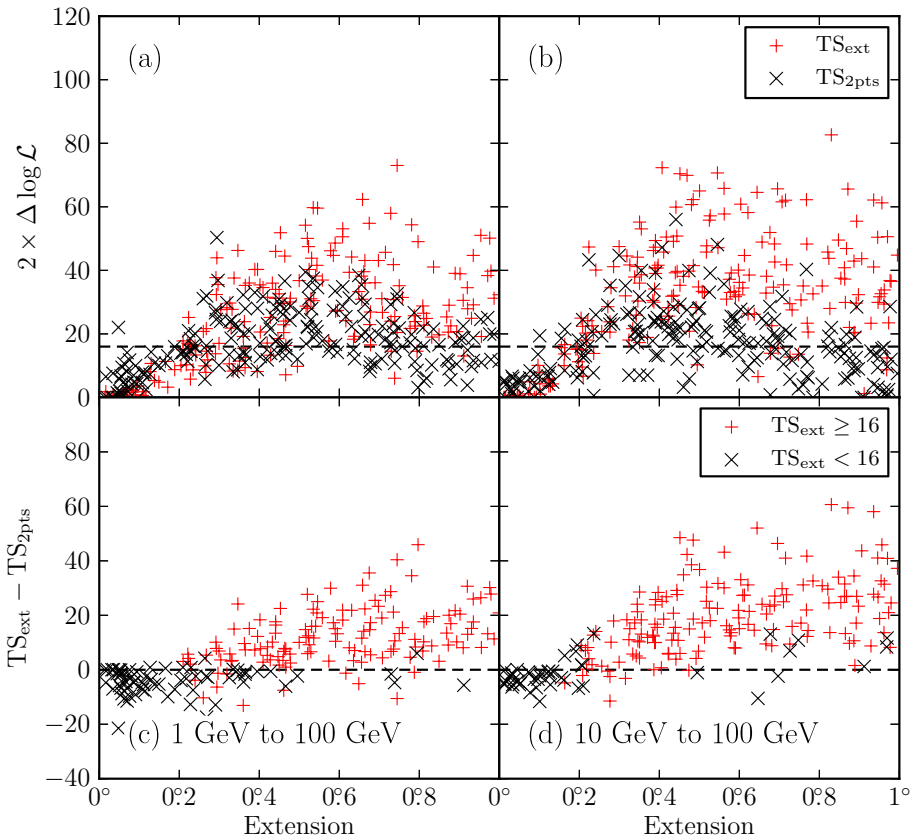

1. Non-nested model comparison
2. Simulate extended sources.
3. Fit as point-like sources.
4. Can easily fit an extended source as two point-like sources

Fig. 9: Effects of Source Confusion (cont)

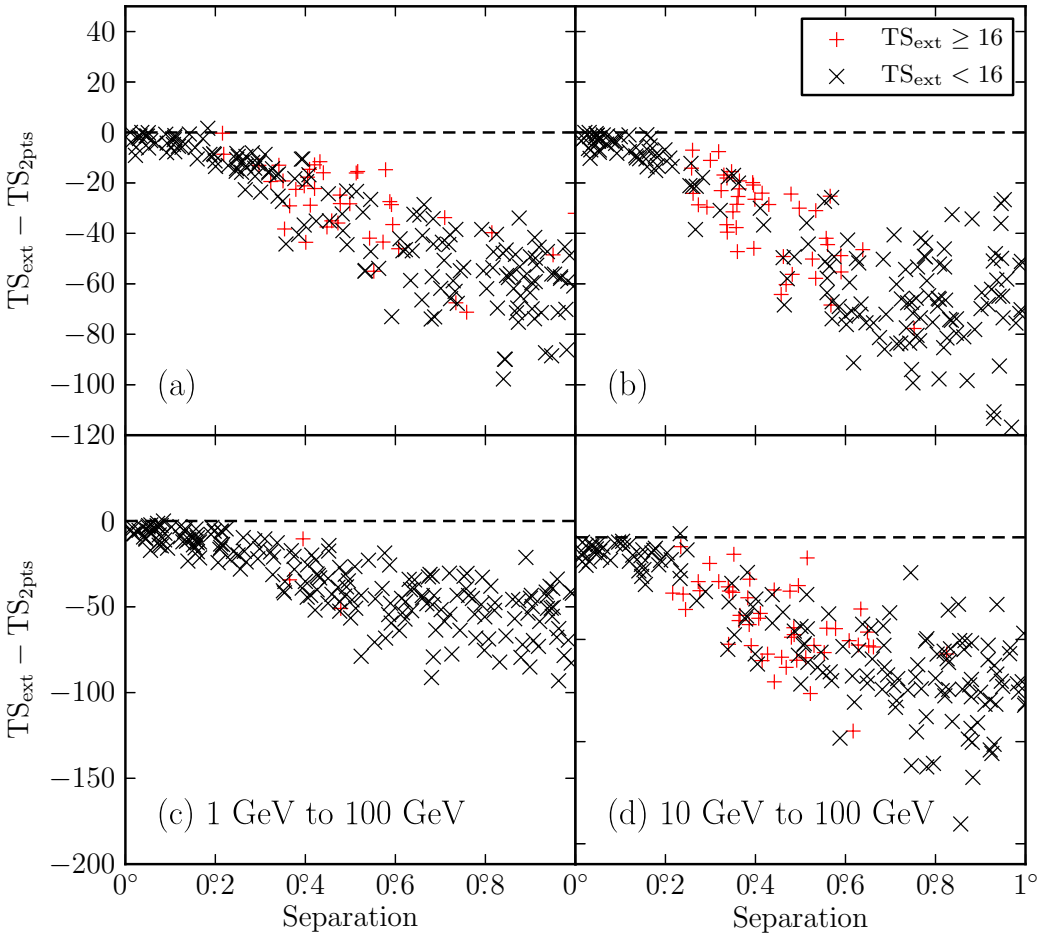

1. Simulate point-like sources.
2. Fit for extension.
3. Not likely to confuse two point-like sources as an extended source

Fig. 10: TS_{EXT} for 2LAC AGN

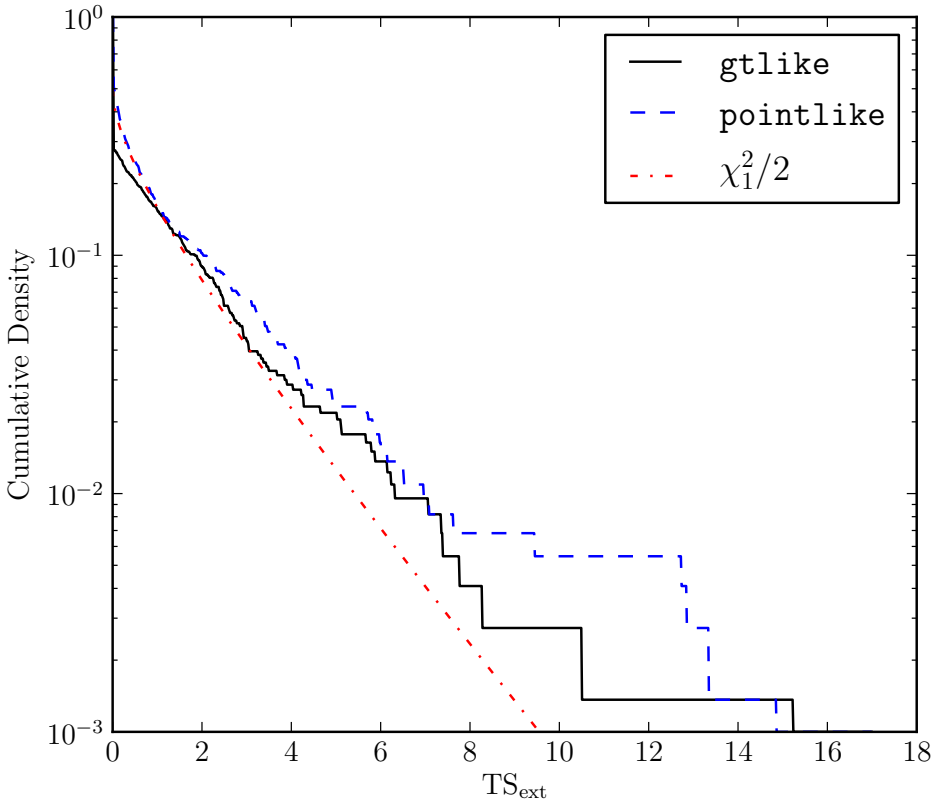

- Use point-like AGN to validate extended source analysis
- Test clean 2LAC AGN for extension
- Don't find AGN to be extended!

Fig. 1 + 11: IC 443

- IC443 is the Most significantly extended source
- Below are diagnostic plots

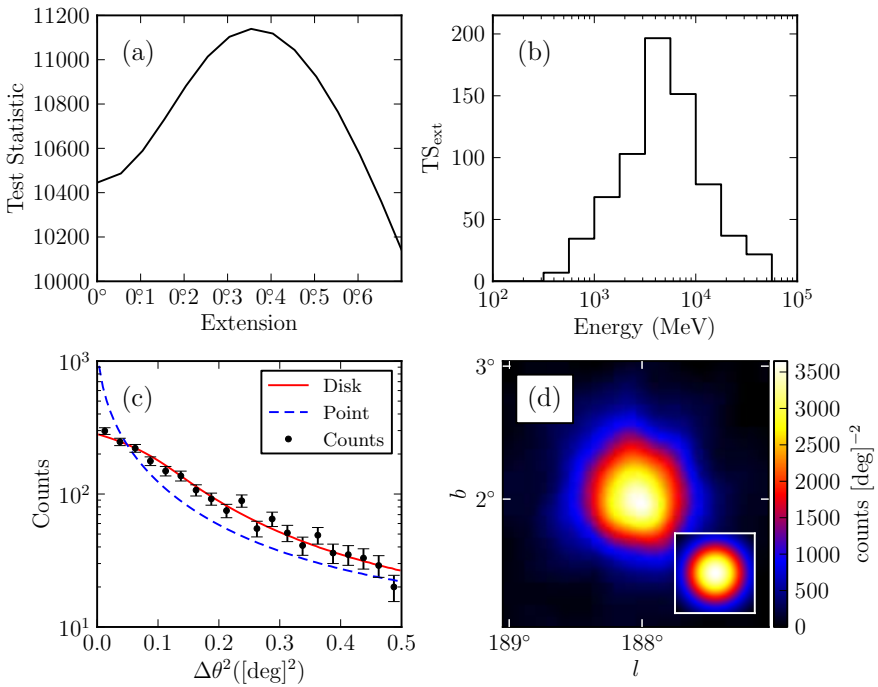

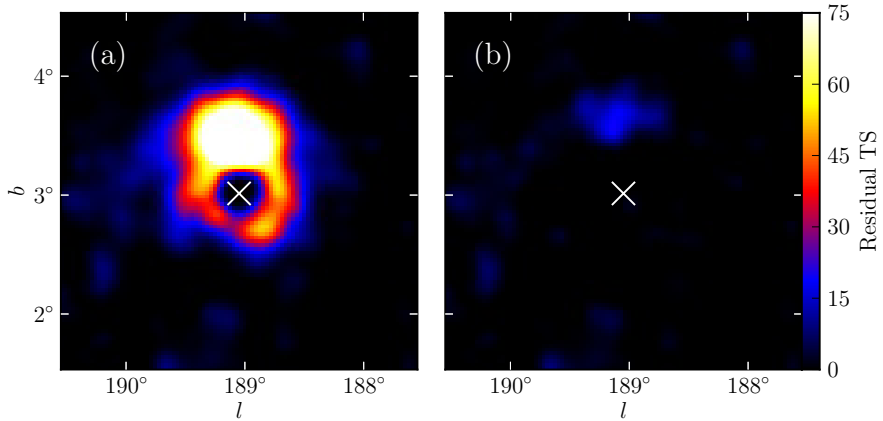

Residual TS Map

- (a) IC443 a point source
- (b) IC443 extended

Table 3: extended sources in 2FGL

Table 3. Analysis of the twelve extended sources included in 2FGL

Name	GLON (deg.)	GLAT (deg.)	σ (deg.)	TS	TS_{ext}	Pos Err (deg.)	Flux[(a)]	Index
			E>1 GeV					
SMC	302.59	-44.42	$1.32 \pm 0.15 \pm 0.31$	95.0	52.9	0.14	2.7 ± 0.3	2.48 ± 0.19
LMC	279.26	-32.31	$1.37 \pm 0.04 \pm 0.11$	1127.9	909.9	0.04	13.6 ± 0.6	2.43 ± 0.06
IC443	189.05	3.04	$0.35 \pm 0.01 \pm 0.04$	10692.9	554.4	0.01	62.4 ± 1.1	2.22 ± 0.02
Vela X	263.34	-3.11	0.88					
Centaurus A	309.52	19.42	~ 10					
W28	6.50	-0.27	$0.42 \pm 0.02 \pm 0.05$	1330.8	163.8	0.01	56.5 ± 1.8	2.60 ± 0.03
W30	8.61	-0.20	$0.34 \pm 0.02 \pm 0.02$	464.8	76.0	0.02	29.1 ± 1.5	2.56 ± 0.05
W44	34.69	-0.39	$0.35 \pm 0.02 \pm 0.02$	1917.0	224.8	0.01	71.2 ± 0.5	2.66 ± 0.00
W51C	49.12	-0.45	$0.27 \pm 0.02 \pm 0.04$	1823.4	118.9	0.01	37.2 ± 1.3	2.34 ± 0.03
Cygnus Loop	74.21	-8.48	$1.71 \pm 0.05 \pm 0.06$	357.9	246.0	0.06	11.4 ± 0.7	2.50 ± 0.10
			E>10 GeV					
MSH15−52	320.39	-1.22	$0.21 \pm 0.04 \pm 0.04$	76.3	6.6	0.03	0.6 ± 0.1	2.20 ± 0.22
HESS J1825−137	17.57	-0.45	$0.65 \pm 0.04 \pm 0.02$	82.9	44.9	0.05	1.8 ± 0.8	1.83 ± 0.73

[(a)]Integral Flux in units of 10^{-9} ph cm^{-2} s^{-1} and integrated in the fit energy range (either 1 GeV to 100 GeV or 10 GeV to 100 GeV).

Note. — All sources were fit using a spatial model assuming a uniform radially symmetric intensity distribution. GLON and GLAT are Galactic longitude and latitude of the best fit extended source respectively. The first error on σ is statistical and the second is systematic (see Section 8). The errors on the integral fluxes and the spectral indices are statistical only. Pos Err is the error on the position of the source. Vela X and the Centaurus A Lobes were not fit in our analysis but are include for completeness.

- Test 12 extended 2FGL sources for extension
- Systematic reanalysis using 2 years of data.
- Assume uniform disk
- Extended sources are extended!

Section 9: Extended Source Search

- Run a dedicated search
- Try to find previously-unresolved extended 2FGL sources
- Search for $E > 1$ GeV and $E > 10$ GeV
- Many difficulties in search, discussed at length in text...
- Publish only good candidates

Fig. 12: Systematics in the plane

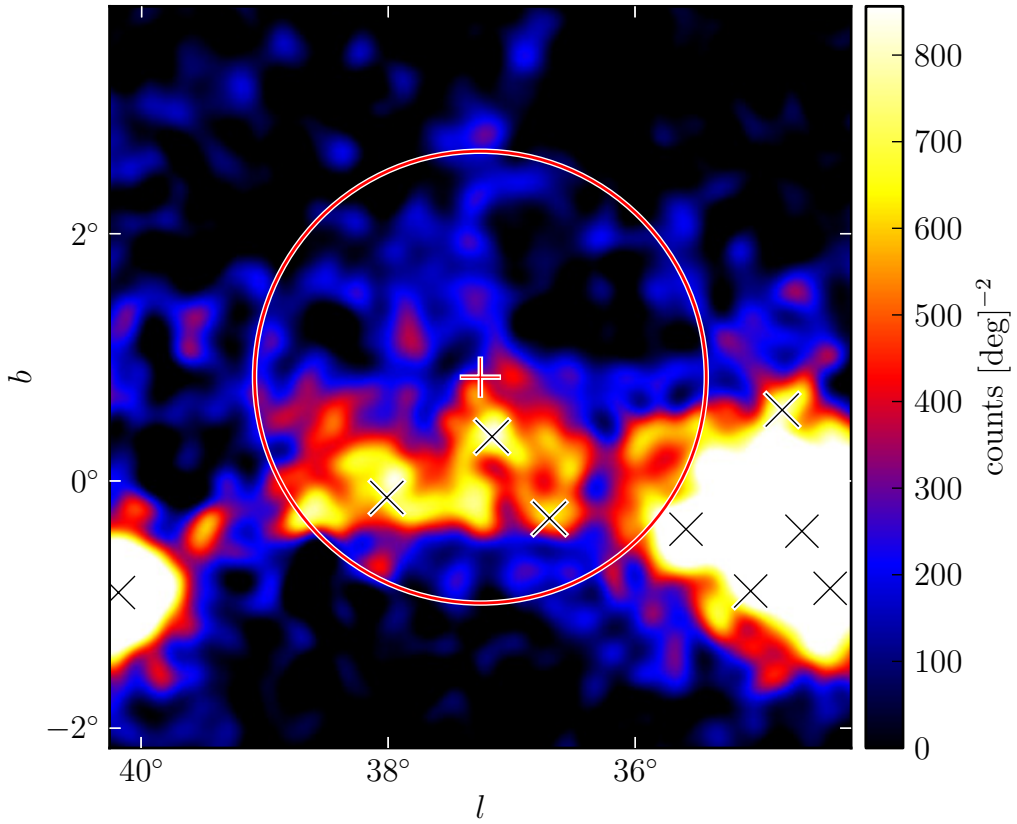

Fig 13: Puppis A

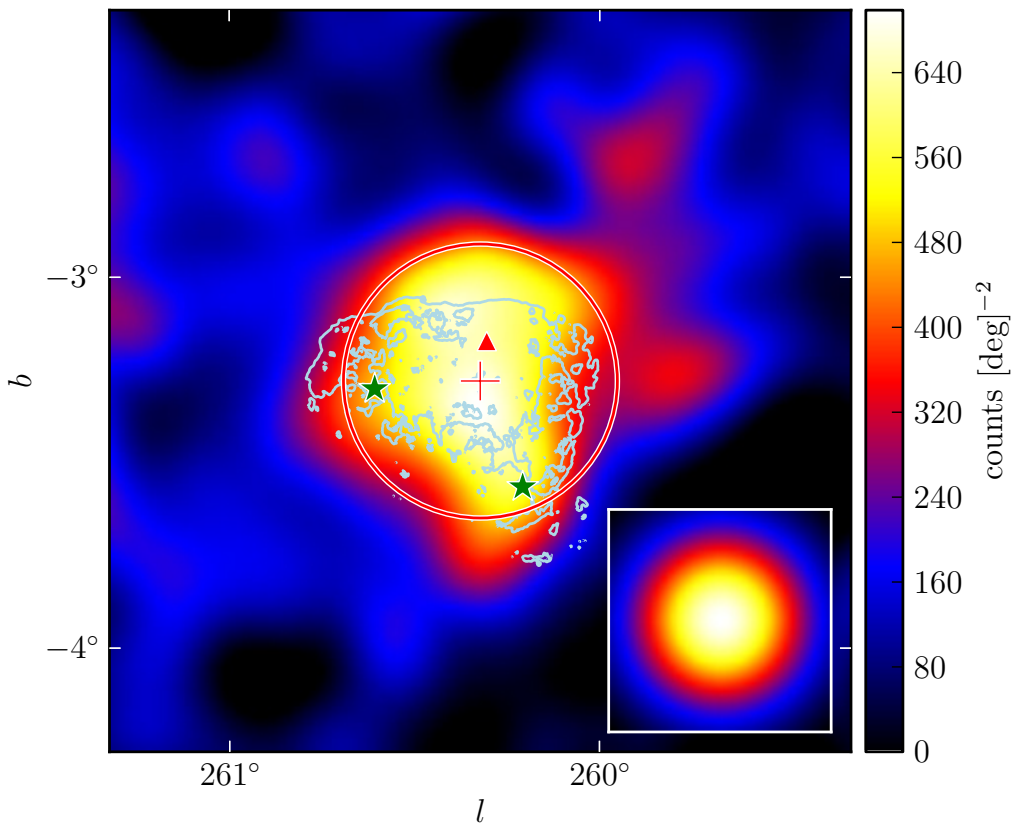

- 1 GeV to 100 GeV
- Middle-aged SNR
- ROSAT X-ray contours (Petre+1996)
- SNR not observed to interact with molecular clouds (Paron+2008)
- Similar to Cygnus Loop

Fig 22: γ-Cygni

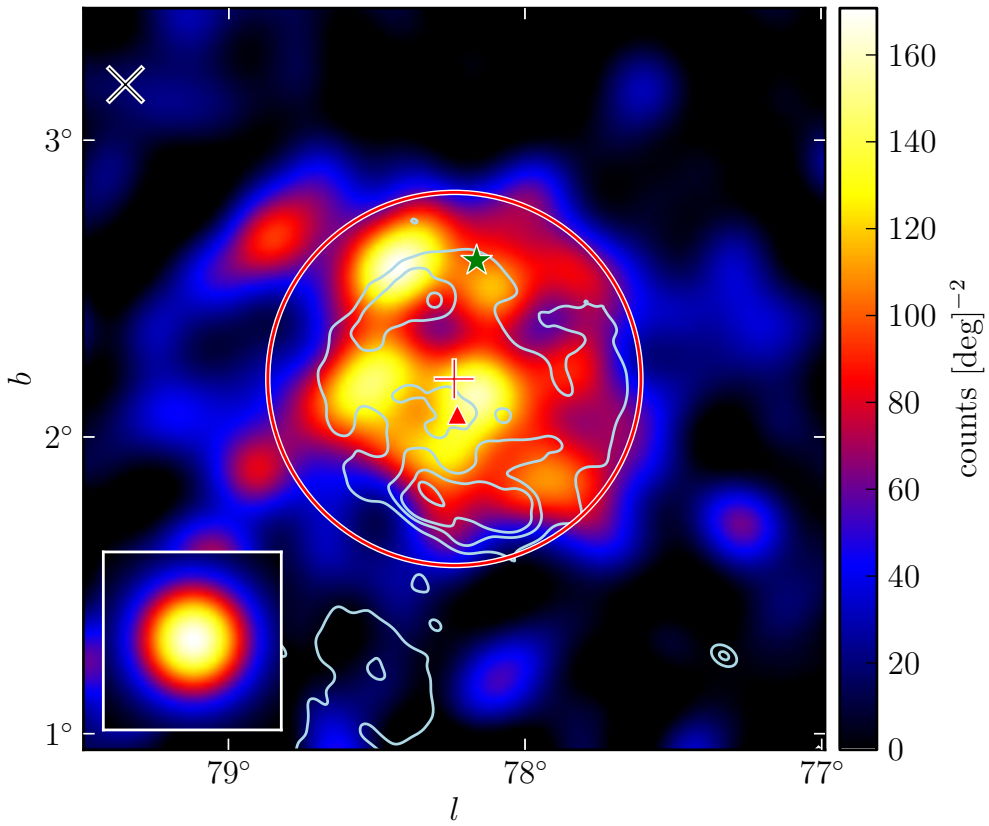

- 10 GeV to 100 GeV
- PSR J2021+4026 at lower energies
- Radio contours (Taylor+2003)
- SNR interacting with Molecular cloud
- Milagro: 4.2σ excess at $\sim$ 30 TeV (Abdo+2009)
- VER J2019+407 detected by Veritas at 200 GeV (Weinstein 2009)

Fig. 14: SED of SNRs

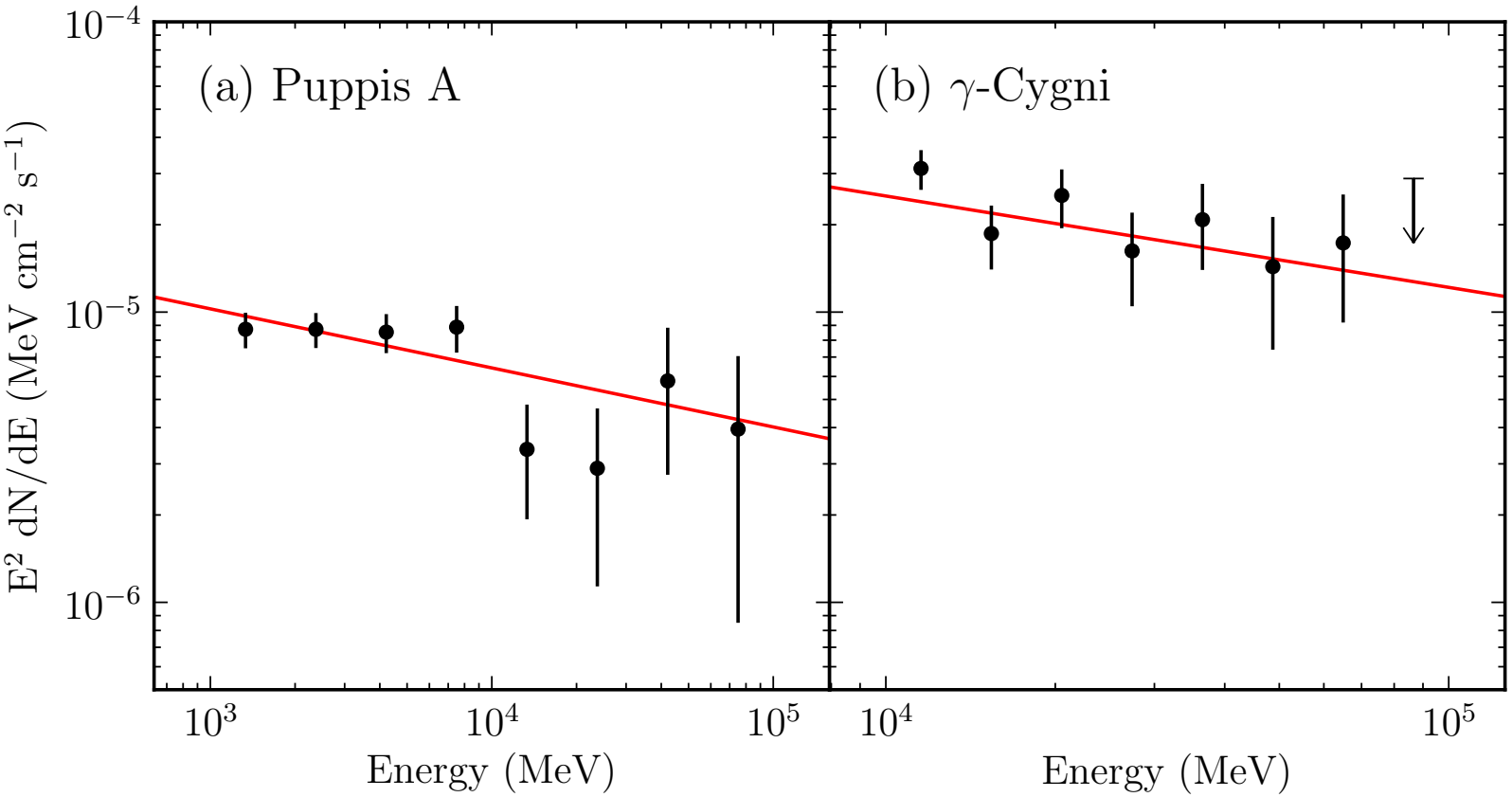

Fig 17. HESS J1614−518 & HESS J1616−508

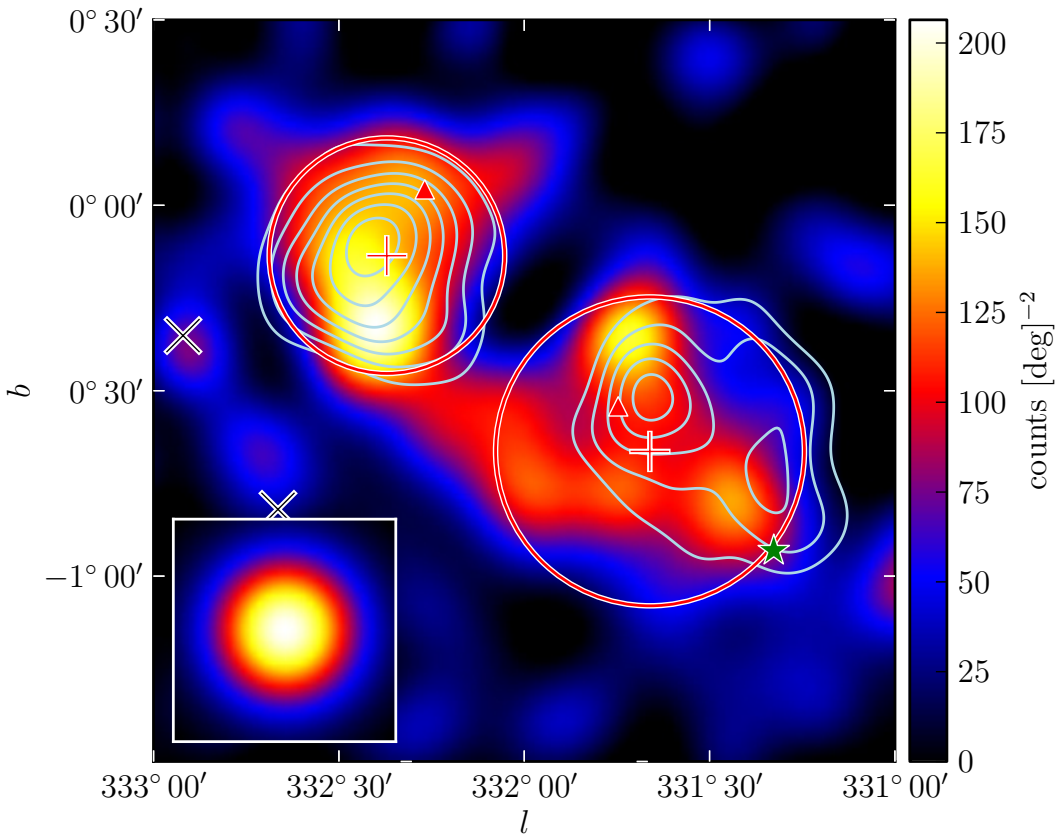

- 10 GeV to 100 GeV
- Two nearby LAT extended sources
- both coincident with extended TeV sources.

- (left): 2FGL J1615.0−5051 → HESS J1616−508
- (right): 2FGL J1615.2−5138 → HESS J1614−518

2FGL J1615.0−5051 → HESS J1616−508

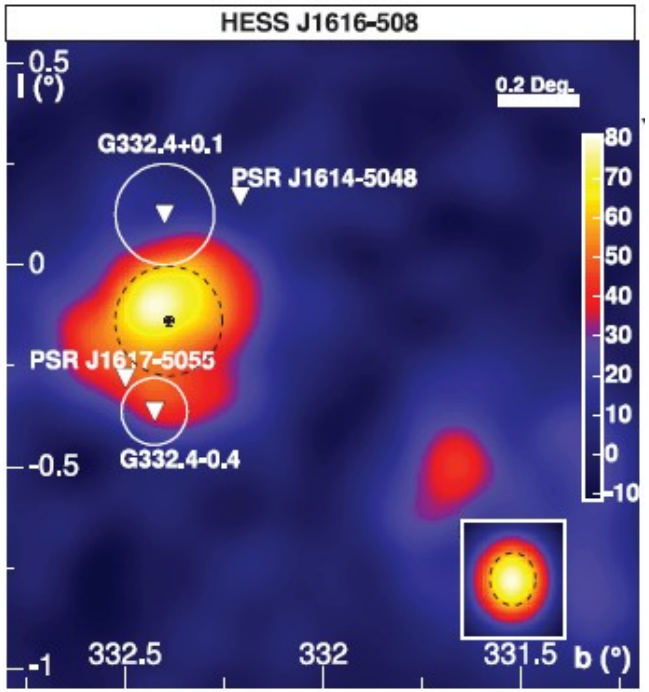

- 2 nearby SNRs: RCW103 and Kes 32 - not spatially coincident (Aharonian+2006)
- 3 Nearby Pulsars: only PSR J1617−5055 energetically powerful enough
  - 9' away → offset PWN?
  - *Chandra* detected $\sim 1'$ PWN
  - not oriented towards HESS J1616−508
- Other diffuse emission in region (Kargaltsev+2009)

2FGL J1615.2−5138 → HESS J1614−518

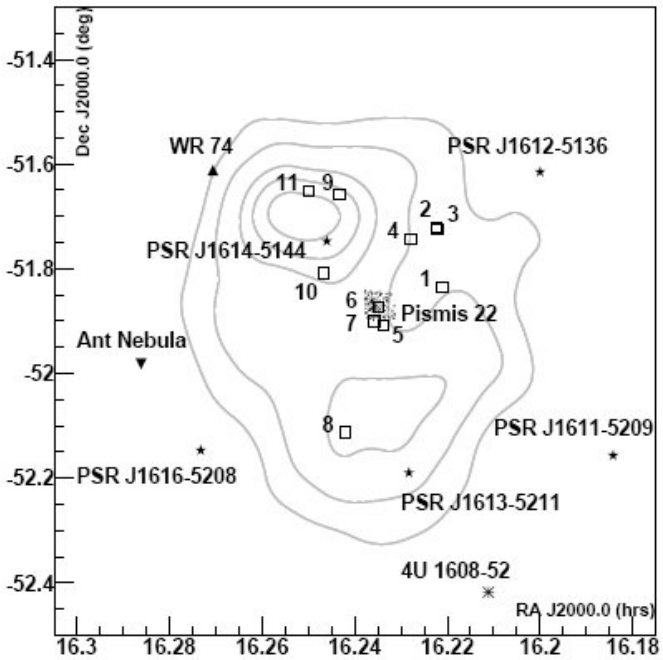

- 5 nearby pulsars, but none powerful enough (Rowell+2008)
- Open cluster Pisim 22
- Suzaku: 2 X-ray sources, one towards peak of HESS J1614−518 and one coincident with Pisim 22 (Matsumoto+2008)
- SNR? PWN? Acceleration in Stellar Winds of Pisim 22?

Fig. 19: HESS J1632-478

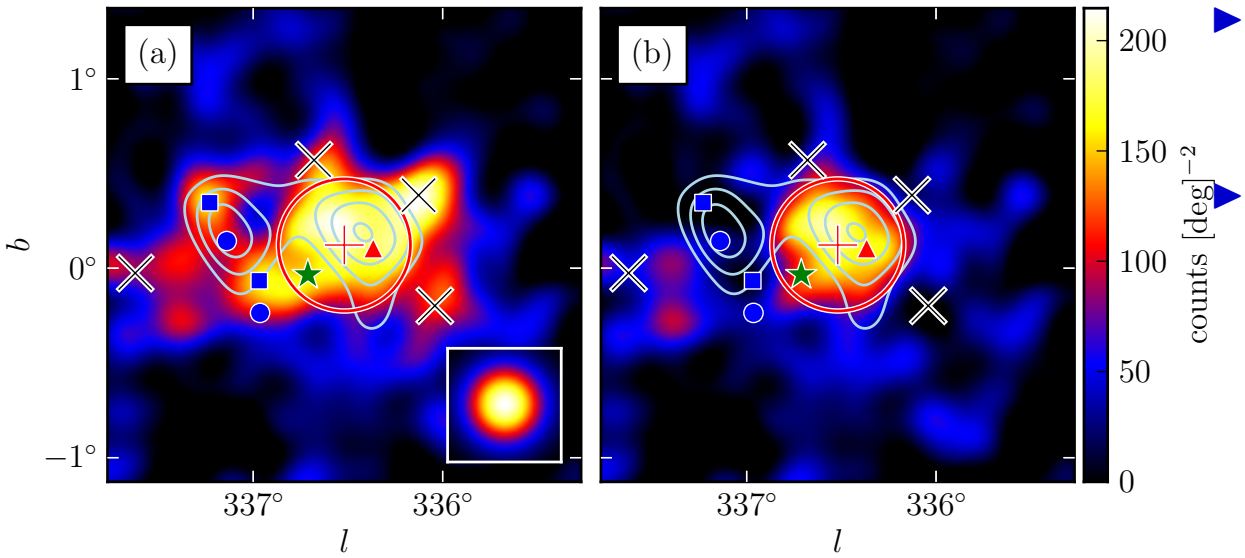

- 10 GeV to 100 GeV
- *XMM-Newton* point-like + extended emission ($32'' \times 15''$)

- PWN? No pulsations (yet) in point-like X-ray source towards center of H.E.S.S source (Balbo+2010)
- Extended radio source in archival MGPS-2 data

Fig. 21: HESS J1837-069

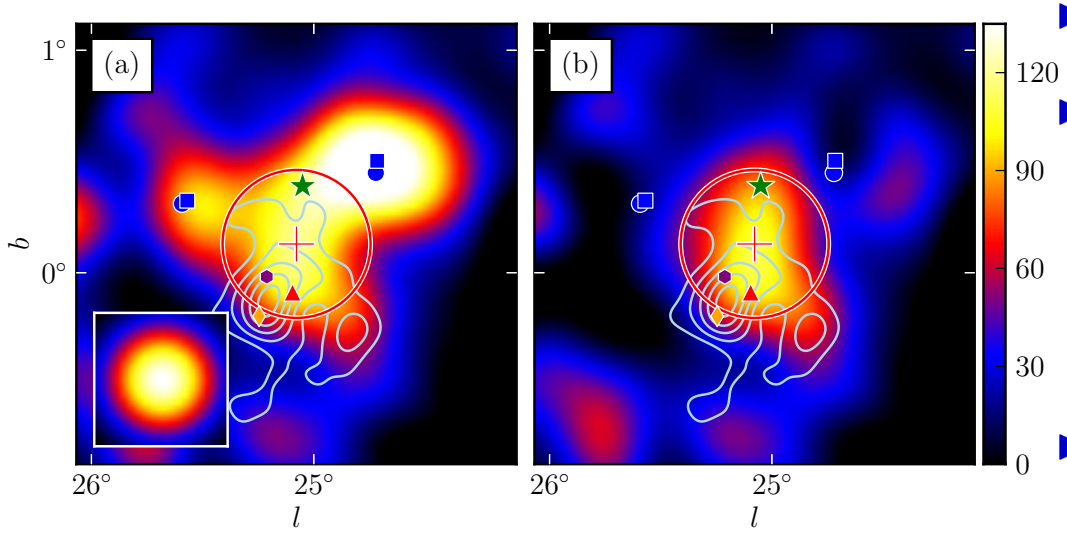

- 10 GeV to 100 GeV
- Coincident with X-ray source AX J1838−0655 (Hertz & Grindlay 1988)
- X-ray Pulsations: PSR J1838−0655

- also: X-ray PWN $\sim 2'$ (Gotthelf & Halpern 2008)
- γ-rays from PWN?
- Second X-ray source AX J1837.3−0652 resolved into point + extended component (no pulsations yet)
- γ-rays from multiple PWN

Fig. 18: SED of HESS Sources

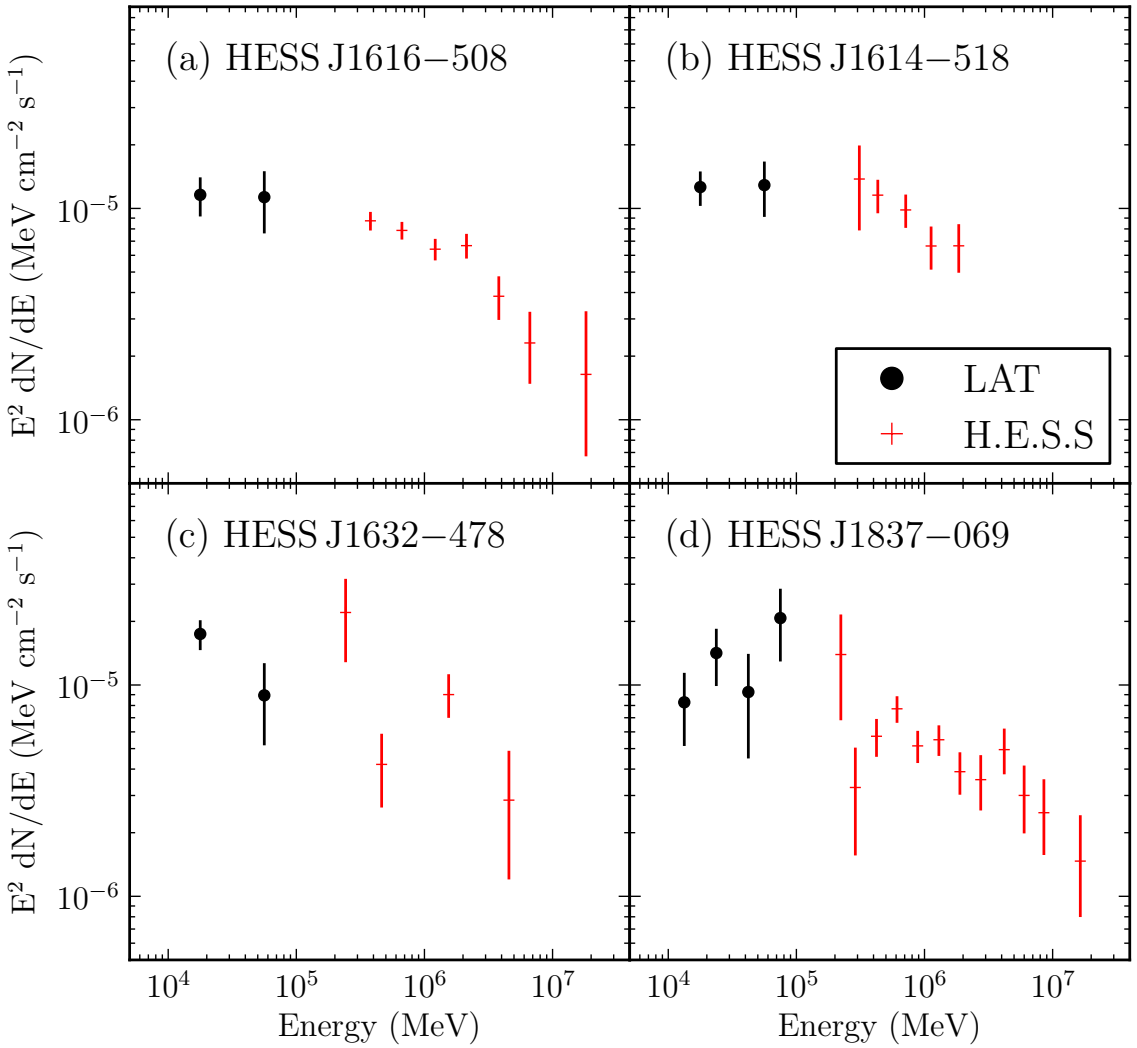

Fig. 20: RX J1713.7−3946

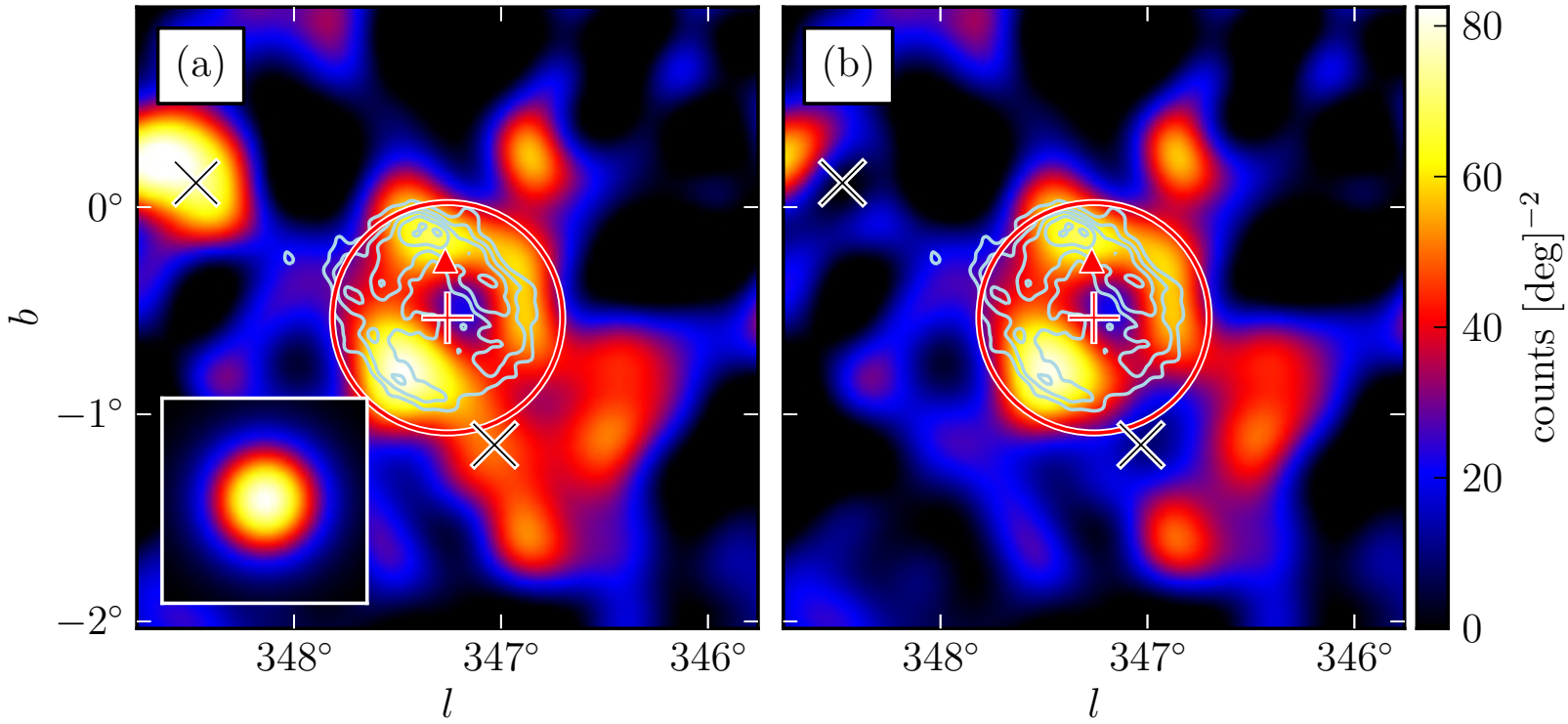

- Beautiful GeV Image for E>10 GeV!

Table 4: New extended Sources

Table 4. Extension fit for the nine additional extended sources

Name	GLON (deg.)	GLAT (deg.)	σ (deg.)	TS	TS_{ext}	Pos Err (deg.)	Flux[a]	Index	Counterpart
				E>1 GeV					
2FGL J0823.0−4246	260.32	−3.28	$0.37 \pm 0.03 \pm 0.02$	322.2	48.0	0.02	8.4 ± 0.6	2.21 ± 0.09	Puppis A
2FGL J1627.0−2425c	353.07	16.80	$0.42 \pm 0.05 \pm 0.16$	139.9	32.4	0.04	6.3 ± 0.6	2.50 ± 0.14	Ophiuchus
				E>10 GeV					
2FGL J0851.7−4635	266.31	−1.43	$1.15 \pm 0.08 \pm 0.02$	116.6	86.8	0.07	1.3 ± 0.2	1.74 ± 0.21	Vela Jr.
2FGL J1615.0−5051	332.37	−0.13	$0.32 \pm 0.04 \pm 0.01$	50.4	16.7	0.04	1.0 ± 0.2	2.19 ± 0.28	HESS J1616−508
2FGL J1615.2−5138	331.66	−0.66	$0.42 \pm 0.04 \pm 0.02$	76.1	46.5	0.04	1.1 ± 0.2	1.79 ± 0.26	HESS J1614−518
2FGL J1632.4−4753c	336.52	0.12	$0.35 \pm 0.04 \pm 0.02$	64.4	26.9	0.04	1.4 ± 0.2	2.66 ± 0.30	HESS J1632−478
2FGL J1712.4−3941[b]	347.26	−0.53	$0.56 \pm 0.04 \pm 0.02$	59.4	38.5	0.05	1.2 ± 0.2	1.87 ± 0.22	RX J1713.7−3946
2FGL J1837.3−0700c	25.08	0.13	$0.33 \pm 0.07 \pm 0.05$	47.0	18.5	0.07	1.0 ± 0.2	1.65 ± 0.29	HESS J1837−069
2FGL J2021.5+4026	78.24	2.20	$0.63 \pm 0.05 \pm 0.04$	237.2	128.9	0.05	2.0 ± 0.2	2.42 ± 0.19	γ-Cygni

[a] Integral Flux in units of 10^{-9} ph cm^{-2} s^{-1} and integrated in the fit energy range (either 1 GeV to 100 GeV or 10 GeV to 100 GeV).

[b] The discrepancy in the best fit spectra of 2FGL J1712.4−3941 compared to Abdo et al. (2011e) is due to fitting over a different energy range.

Section 8: Extension Systematics

Test systematics due to not knowing PSF

- Compare best fit extension to MC based PSF
- Use difference as systematic
- Small effect on extension, large effect on statistical significance
- Probably too conservative...

Test systematics due to not knowing PSF

- Break up GALPROP diffuse model into multiple components
- Fit each component locally
- Tests systematics due to imperfect diffuse modeling

Table 5: Dual Localization, alternate PSF, alternate Diffuse

Table 5. Dual localization, alternative PSF, and alternative approach to modeling the diffuse emission

Name	$TS_{\texttt{pointlike}}$	$TS_{\texttt{gtlike}}$	$TS_{alt,diff}$	$TS_{ext\,\texttt{pointlike}}$	$TS_{ext\,\texttt{gtlike}}$	$TS_{ext\,alt,diff}$	σ (deg.)	$\sigma_{alt,diff}$ (deg.)	$\sigma_{alt,psf}$ (deg.)	TS_{2pts}
				E>1 GeV						
2FGL J0823.0−4246	331.9	322.2	356.0	60.0	48.0	56.0	0.37	0.39	0.39	23.0
2FGL J1627.0−2425c	154.8	139.9	105.7	39.4	32.4	24.8	0.42	0.40	0.58	24.5
				E>10 GeV						
2FGL J0851.7−4635	115.2	116.6	123.1	83.9	86.8	89.8	1.15	1.16	1.17	15.5
2FGL J1615.0−5051[(a)]	48.2	50.4	56.6	15.2	16.7	17.8	0.32	0.33	0.32	13.1
2FGL J1615.2−5138	75.0	76.1	83.8	42.9	46.5	54.1	0.42	0.43	0.43	35.1
2FGL J1632.4−4753c	64.5	64.4	66.8	23.0	26.9	25.5	0.35	0.36	0.37	10.9
2FGL J1712.4−3941	59.8	59.4	39.9	38.4	38.5	30.7	0.56	0.55	0.53	2.7
2FGL J1837.3−0700c	44.5	47.0	39.2	17.6	18.5	16.1	0.33	0.32	0.38	10.8
2FGL J2021.5+4026	239.1	237.2	255.8	139.1	128.9	138.0	0.63	0.65	0.59	37.3

[(a)]Using `pointlike`, TS_{ext} for 2FGL J1615.0−5051 was sligthly below 16 when the source was fit in the 10 GeV to 100 GeV energy range. To confirm the extension measure, the extension was refit in `pointlike` using a slightly lower energy. In the 5.6 GeV to 100 GeV energy range, we obtained a consistent extension and TS_{ext} =28.0. In the rest of this paper, we quote the $E > 10$GeV results for consistency with the other sources.

Fig 23: Skymap of Extended Sources

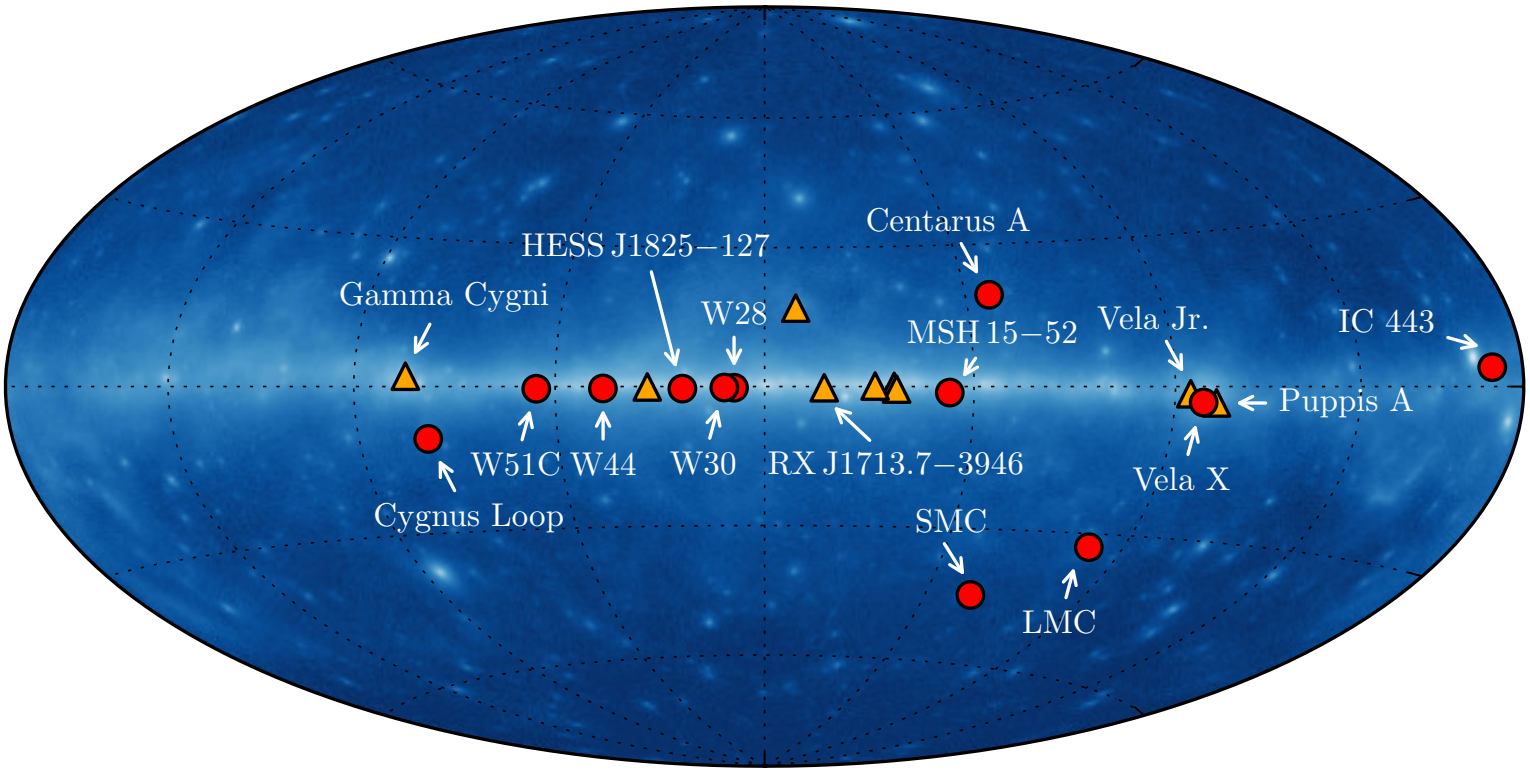

Fig 24: Compare GeV and TeV Sizes

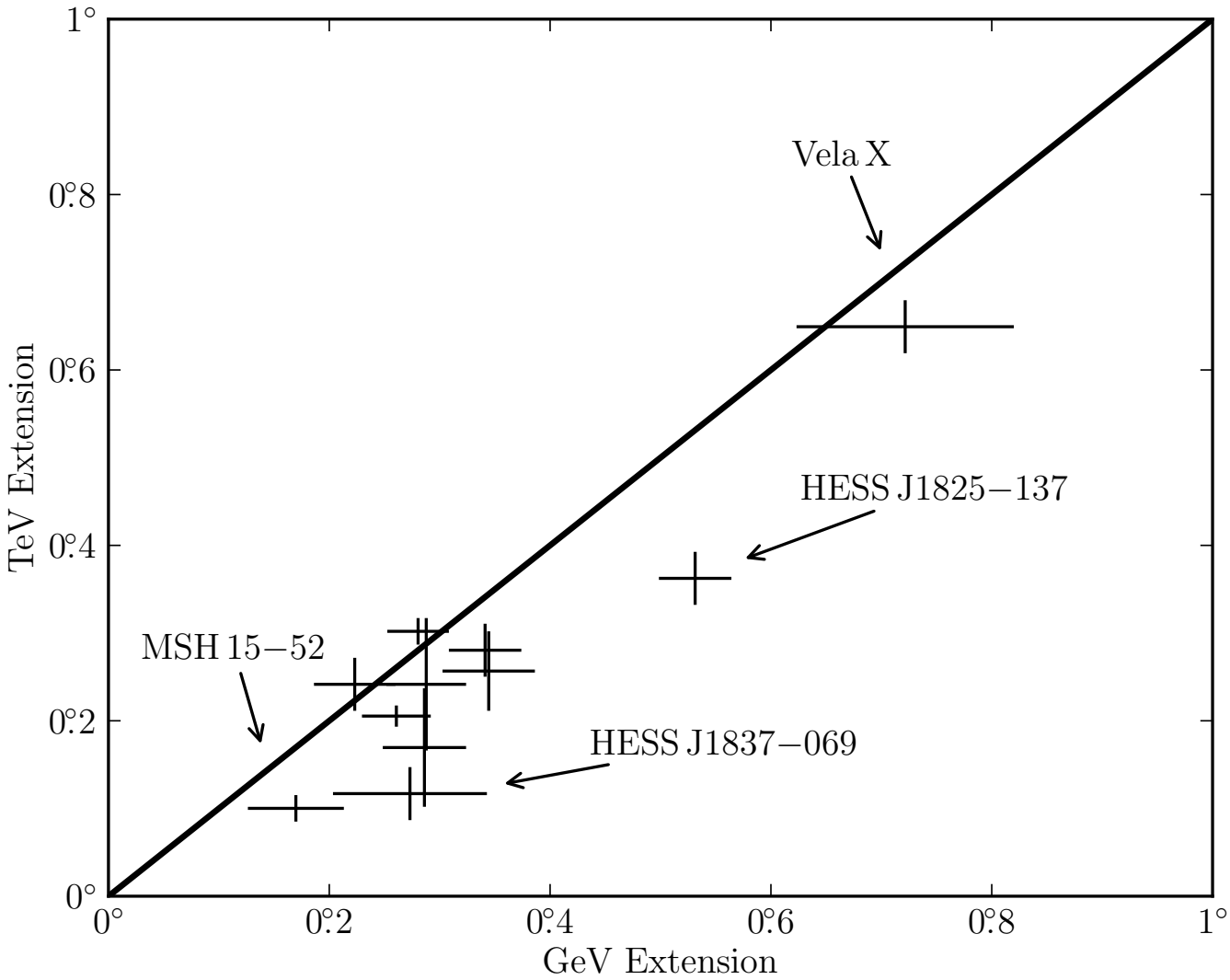

Fig 25: GeV and TeV Sizes (cont)

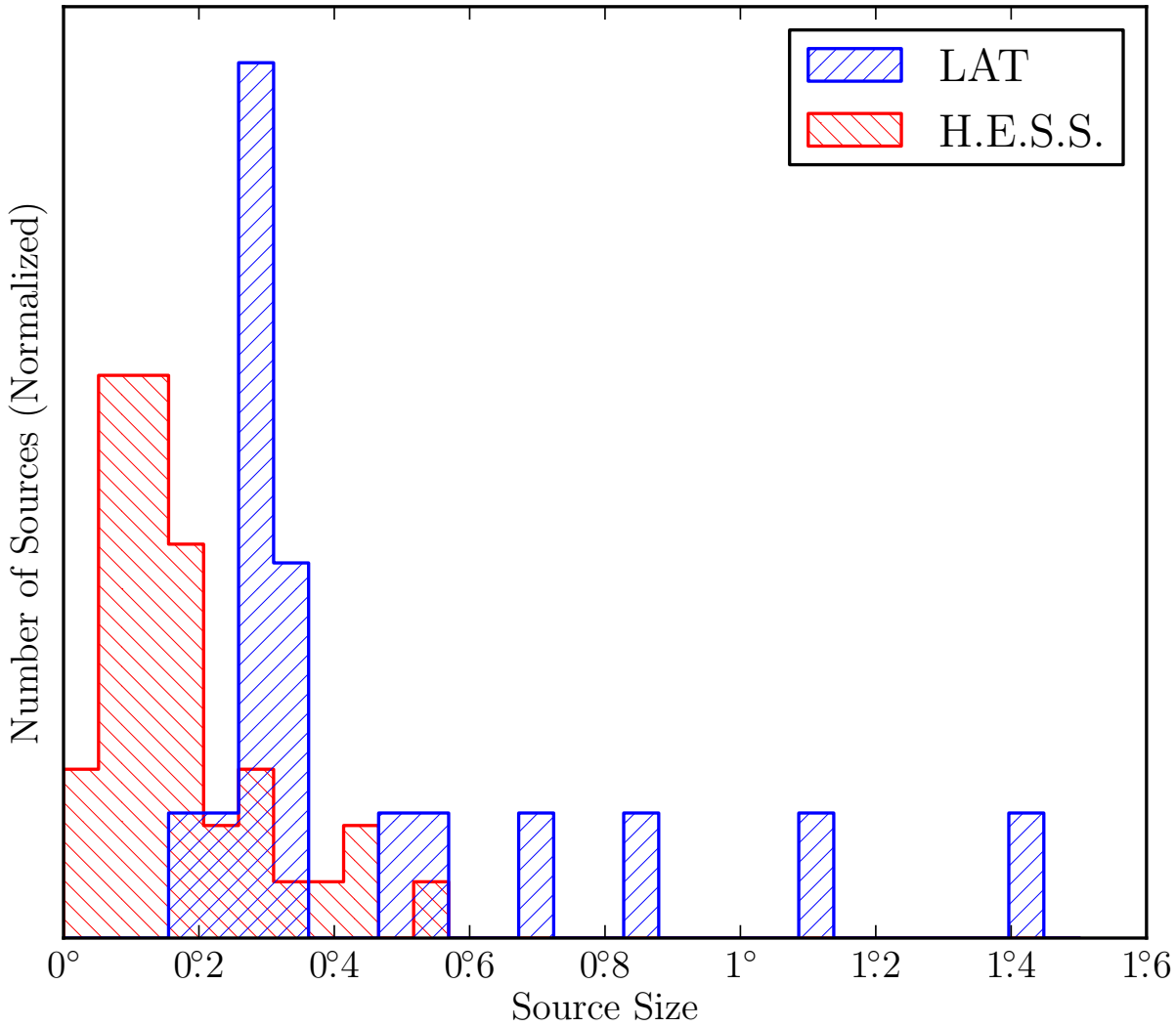

Fig 26: Distribution of Spectral Indices

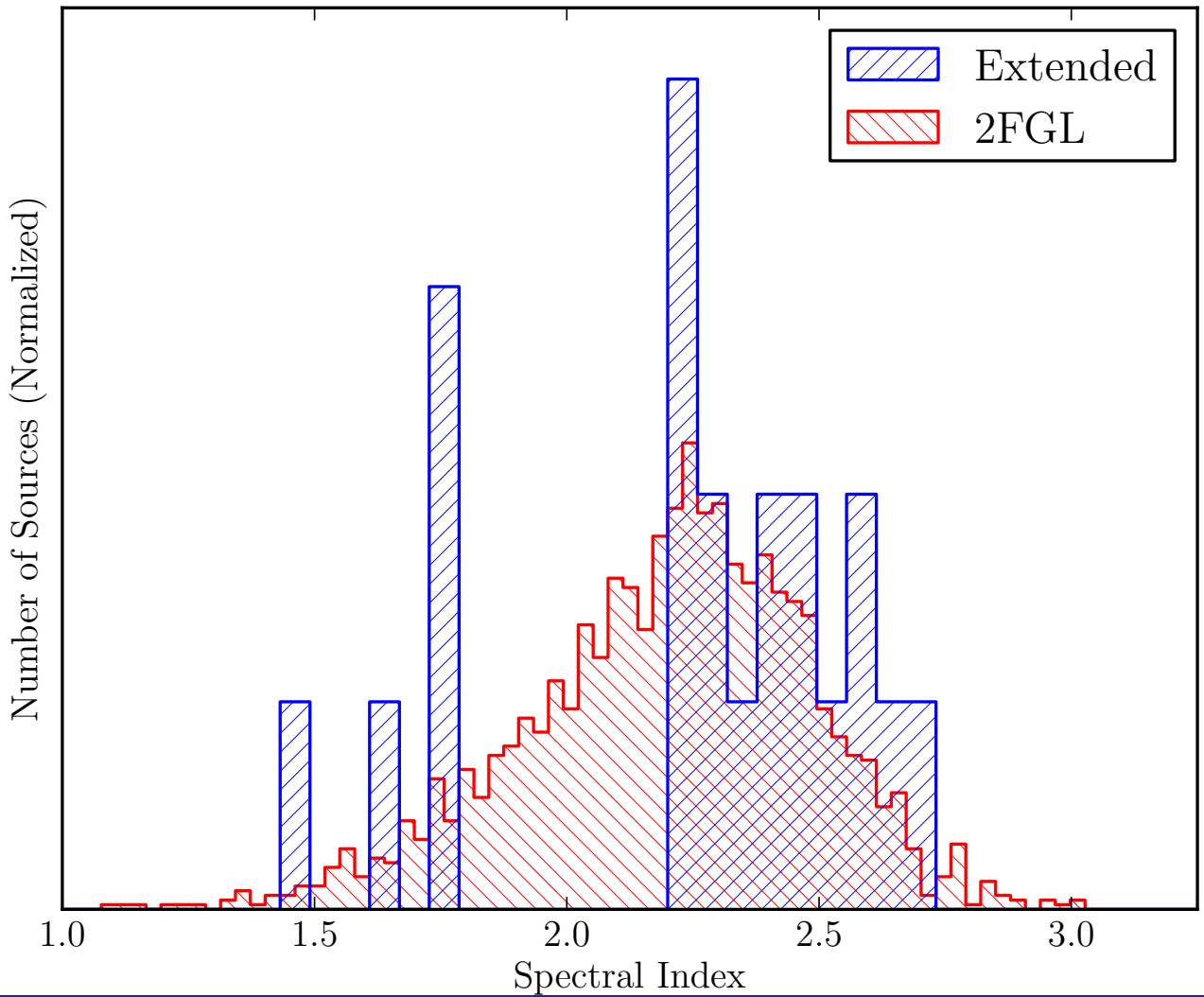

Thank you

See text for more details:

- https://www-glast.stanford.edu/cgi-prot/pub_download?id=662